CEA/SACLAY
DSM

SERVICE DE PHYSIQUE NUCLEAIRE

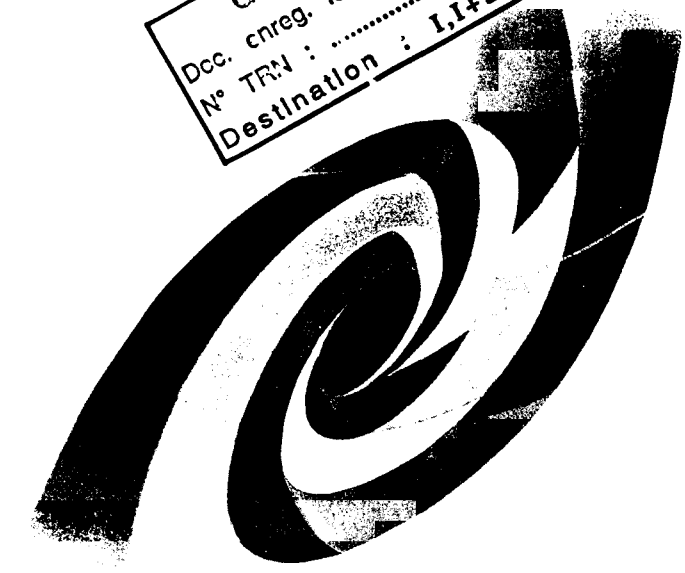

DAPNIA/SPhN-96-28
INC-40007-111

09/1996

Dynamics of GeV light-ion-induced reactions

K. Kwiatkowski, D.S. Bracken, E. Renshaw Foxford, D.S. Ginger,
W.-C. Hsi, K.B. Morley, V.E. Viola, G. Wang, K.G. Korteling,
R. Legrain, E.C. Pollacco, C. Volant.

DAPNIA

Couverture : Sylvie Cabrit et Marc Sauvage

Département d'Astrophysique, de Physique des Particules, de Physique Nucléaire et de l'Instrumentation Associée
CEA/Saclay F-91191 Gif-sur-Yvette Cédex

CEA/SACLAY
DSM

DAPNIA/SPhN-96-28
INC-40007-111

09/1996

Dynamics of GeV light-ion-induced reactions

K. Kwiatkowski, D.S. Bracken, E. Renshaw Foxford, D.S. Ginger,
W.-C. Hsi, K.B. Morley, V.E. Viola, G. Wang, K.G. Korteling,
R. Legrain, E.C. Pollacco, C. Volant.

DAPNIA

Département d'**A**strophysique, de Physique des **P**articules, de Physique **N**ucléaire et de l'**I**nstrumentation **A**ssociée
CEA/Saclay F-91191 Gif-sur-Yvette Cédex

1st Catania Relativistic Ion Studies : Critical Phenomena and Collective Observables, Acicastello, Italy, May 27-31, 1996

INC-40007-111

DYNAMICS OF GeV LIGHT-ION-INDUCED REACTIONS

K. Kwiatkowski, D.S. Bracken, E. Renshaw Foxford[1], D.S. Ginger,
W.-C. Hsi, K.B. Morley[2], V.E. Viola, G. Wang
Departments of Chemistry and Physics and IUCF
Indiana University
Bloomington, IN 47405

R.G. Korteling
Department of Chemistry
Simon Fraser University
Burnaby, BC, Canada

R. Legrain, E. C. Pollacco, C. Volant
CEA/DAPNIA
SPhN, C.E. Saclay
91191 Gif-sur-Yvette
Cedex, France

June, 1996

Primary funding provided by the U.S. Department of Energy; additional support provided by the U.S. National Science Foundation, the National Science and Energy Research Council of Canada, the Commissariat à l'Energie Atomique of France and Indiana University.

---

[1]Present address: Microsoft Corp., Seattle, WA
[2]Present address: Los Alamos National Laboratory, Los Alamos, NM

DYNAMICS OF GeV LIGHT-ION-INDUCED REACTIONS

K. KWIATKOWSKI, D.S. BRACKEN, E. RENSHAW FOXFORD, D.S. GINGER, W.-C. HSI, K.B. MORLEY, V.E. VIOLA, G. WANG
Departments of Chemistry and Physics and IUCF, Indiana University, Bloomington, IN 47405

R.G. KORTELING
Department of Chemistry, Simon Fraser University, Burnaby, BC, Canada

R. LEGRAIN, E. C. POLLACCO, C. VOLANT
CEA DAPNIA/SPhN, C.E. Saclay, 91191 Gif-sur-Yvette, Cedex, France

Recent results from studies of the 1.8 - 4.8 GeV ^{3}He + ^{nat}Ag, ^{197}Au reactions at LNS with the ISiS detector array have shown evidence for a saturation in deposition energy and multifragmentation from a low-density source. The collision dynamics have been examined in the context of intranuclear cascade and BUU models, while breakup phenomena have been compared with EES and SMM models. Fragment-fragment correlations support a model in which multifragmentation is a time-dependent phenomenon that occurs on a short < 100 fm/c time scale. Isotope-ratio temperatures exhibit features of the "caloric curve" of Pochodzalla *et al.*, but these are dependent on angle of observation and selection of fragment energy gates.

1 Introduction

The heating of finite nuclear matter to temperatures in the vaporization regime can be achieved via two primary pathways. Most common–and the subject of most papers at this conference–involves compressional heating in heavy-ion collisions. Alternatively, high temperatures can also be reached in central light-ion-induced reactions on heavy nuclei as a consequence of hard N-N collisions, supplemented by the excitation of multiple delta resonances and pion reabsorption. The latter approach is the subject of this report.

Recently, our group has conducted a series of light-ion studies with the Indiana Silicon Sphere 4π charged-particle detector array.[1] The objectives of these studies have been to investigate transport phenomena and the disintegration of the hot residues formed in these collisions, as well as the important nonequilibrium processes that link the initial and final stages of the reaction. Particular attention has been devoted to characterizing the thermal properties of the disintegrating systems. This experimental program has spanned the intermediate-energy region, extending from (1) the Fermi-energy domain at IUCF (E375: 130 - 270 MeV p and ^{3}He beams) to (2) reactions in the vicinity

of the Δ resonance at LNS (E228: 1.8 - 4.8 GeV ^{3}He) to (3) the limiting fragmentation region at AGS (E900: 5.0 - 14.6 GeV/c p, π^-). The lower-energy studies have focussed on nonequilibrium processes and those at higher energies on multifragmentation and its relation to the nuclear equation of state. This report will emphasize the results from LNS,[2,3] which were obtained with 1.8 - 4.8 GeV ^{3}He incident on silver and gold nuclei.

Simulations of the ^{3}He reaction dynamics with both intranuclear cascade (INC)[4] and BUU models[5-7] predict that energy deposition occurs on a time scale of 20 - 30 fm/c and that by 40 fm/c, the entropy per nucleon is nearly constant, indicating the residue has entered the chaotic regime. At this time, the maximum deposition energy is predicted to be $E^* \sim 10-12$ MeV/nucleon. In addition, both INC[8] and BUU calculations[7] indicate that for central collisions, a region of depleted density develops in the center of the nucleus as a consequence of the fast cascade. When fluctuations are folded in, this provides a mechanism for destabilization of the system and subsequent multifragmentation.

2 Energy Deposition

In order to gauge the deposition energy in these reactions, we have examined several experimental variables. One of the most important of these is the multiplicity of intermediate-mass fragments (IMF: $3 \leq Z \lesssim 20$), which is believed to be strongly correlated with excitation energy.[9-11] The experimental multiplicity distributions scale systematically with target mass and bombarding energy.[2] However, for the 3.6 and 4.8 GeV ^{3}He+^{nat}Ag reactions, the multiplicity distributions are identical, suggesting that a saturation of deposition energy has been achieved. This is predicted by both INC and BUU calculations[7] and is understood in terms of the forward-focussing and increased momentum of the secondary pions, which reduce their absorption probability.

In contrast to the IMF multiplicities, the light-charged-particle (LCP) distributions extend to higher values at 4.8 GeV than at 3.6 GeV for the ^{nat}Ag target. To understand this, we have examined the fragment energy spectra. In Fig. 1, energy spectra for He, Li and C fragments observed at 14° - 22° are shown for events with two or more IMFs. The significant yields of energetic LCPs and IMFs are apparent and demonstrate that even for high deposition-energy events, nonequilibrium processes compose an important fraction of the yield. The dashed lines in Fig. 1 indicate the maximum contributions from equilibrium-like emission, as determined from two-source fits to the data at all angles.

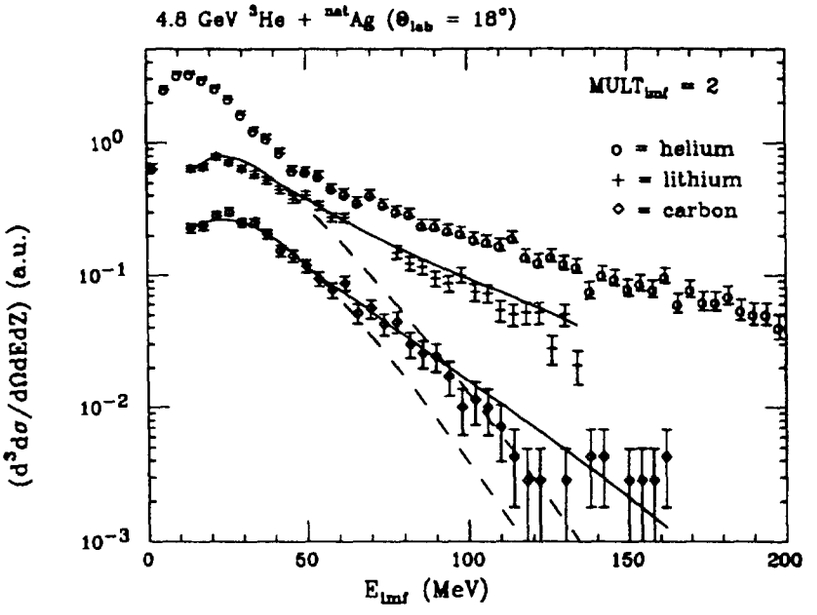

Figure 1: Spectra of He, Li, and C fragments for M_{IMF} = 2 events at 14° - 22°. Data are from 4.8 Gev ^{3}He + ^{nat}Ag system. Solid lines are two-component moving source fits to the Li and C spectra; dashed lines represent the corresponding slow component.

To investigate the effect of nonequilibrium emission on excitation-energy gauges, we have schematically separated all spectra into thermal and fast components. For each Z value, thermalized charged particles are defined as those ejectiles with energies ϵ^i_{th} below a cutoff energy,

$$\epsilon^{max}_{th} = C_o \bullet Z_f + \epsilon_0, \quad (1)$$

where C_o is a parameter corresponding to the peak of the inclusive energy spectrum for each fragment charge, Z_f, and ϵ_0 = 31 MeV. All ϵ_{th} values are calculated in the moving-source reference frame and the cutoff energy ϵ^{max}_{th} corresponds approximately to the discontinuity in the slope of the spectra tails in Fig. 1.

The above separation permits calculation of an energy sum that minimizes nonequilibrium contributions and is directly related to the excitation energy of each multifragmentation event. This quantity is defined as the total thermalized energy

$$E_{th} = \Sigma_i \epsilon^i_{th} (\epsilon^i < \epsilon^{max}_{th}). \quad (2)$$

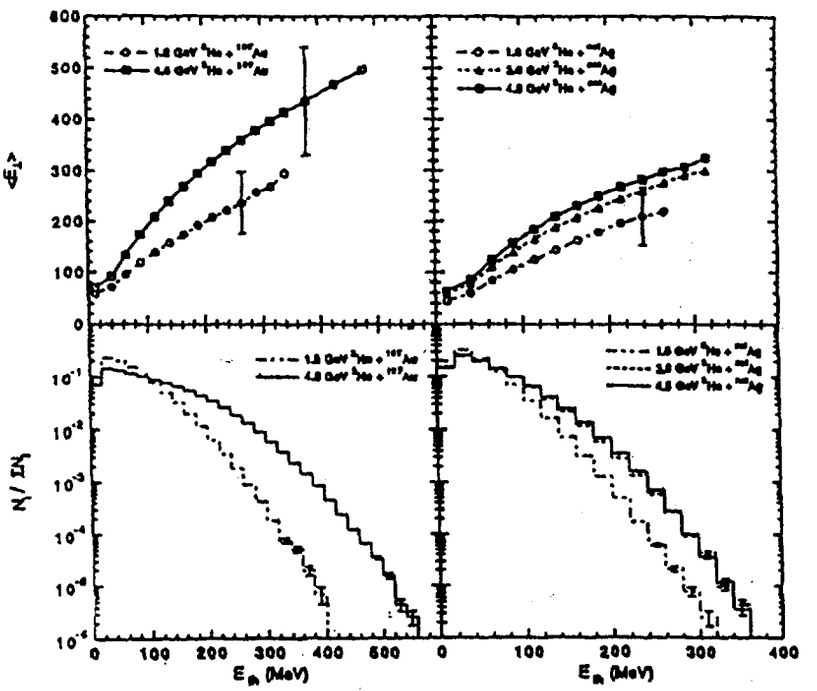

Figure 2: Lower frames: Distributions of observed total thermalized energy per event for ^{3}He + ^{197}Au (left) and ^{3}He + ^{nat}Ag (right); upper frames: Correlation between total themalized energy and transverse energy. Error bars indicate standard deviations of distribution widths ($\pm$ σ) and are representative of data. Systems are defined on figure.

The E_{th} distributions shown in Fig. 2 exhibit the same features as the IMF multiplicity distributions; i.e. E_{th} scales with target mass and projectile energy–except the 3.6 and 4.8 GeV ^{3}He + Ag systems give identical results. This provides an independent confirmation of the saturation in deposition energy for the ^{3}He + Ag reaction. At the 10^{-6} probability level, the maximum observed values of E_{th} translate into maximum deposition energies of the order of 950 MeV for Ag residues and 1600 MeV for ^{197}Au, when corrected for solid angle, neutron emission and binding energies. Allowing for mass loss during the fast cascade,[4] these deposition energies correspond to $E^*/A \sim 12$ MeV for the Ag target and $E^*/A \sim 10$ MeV for Au. These values are in good agreement with predictions of the INC model.[4]

In summary, two classes of reaction observables emerge from the above analysis, one related to the excitation energy of the thermalized source and the other more characteristic of projectile energy dissipation, which includes nonequilibrium processes. In the former group, the multiplicities of IMFs and thermalized particles, the total thermalized energy, and the total observed charge all behave similarly and appear to be reliable deposition energy gauges. In contrast, significant nonequilibrium contributions are included in observables such as the LCP and total charge-particle multiplicities and the transverse energy distribution (shown in Fig. 2).

3 Breakup Dynamics

The breakup dynamics of the highly excited residues formed in GeV ^{3}He-induced reactions have been examined in several contexts. Both rapidity analyses and moving-source fits to the spectra of all IMFs indicate the presence of two sources: a dominant equilibrium-like source and a smaller nonequilibrium source.[2,3] The equilibrium-like source appears to involve isotropic emission and kinetic energy spectra with peaks that broaden and shift to lower energies with increasing collision violence. This latter result has been interpreted[3,12] as direct evidence for emission from a source expanded to a density $\rho/\rho_0 \leq 1/3$. In addition, both small-angle correlations and coplanarity-sphericity analyses lead to the conclusion that the breakup mechanism is fast; the former favors a simultaneous breakup scenario[3] and the latter yields emission times < 50 fm/c for the most violent events.[12]

In an effort to understand the time evolution of the breakup process we have examined large-angle correlations ($\theta = 180° \pm 40°$) for fragments with identical charges. These distributions are sensitive to the Coulomb field of the emitting source, and thus reflect its size and charge.

In Fig. 3 the relative velocity distributions are shown for several identical fragment pairs, along with those for all possible fragment pairs. The results show a systematic evolution toward lower relative velocities as the fragment charge increases. For the heaviest fragments, the relative velocites are in good agreement with fission systematics, for which a value of $r_0 \sim 1.8$ fm accounts for the separation distance between binary fragments. [When compared to a value of r_o for nuclei of 1.2 fm, this would correspond to a density of $\rho/\rho_o \approx 1/3$]. With decreasing IMF charge, the centroids of the relative velocity distriubtion diverge significantly above the Coulomb energy for fission.

The relative velocity results have been compared with predictions based on two different models: the expanding emitting source model (EES) of Friedman,[9] and the statistical multifragmentation (SMM) model of Botvina.[13] The EES

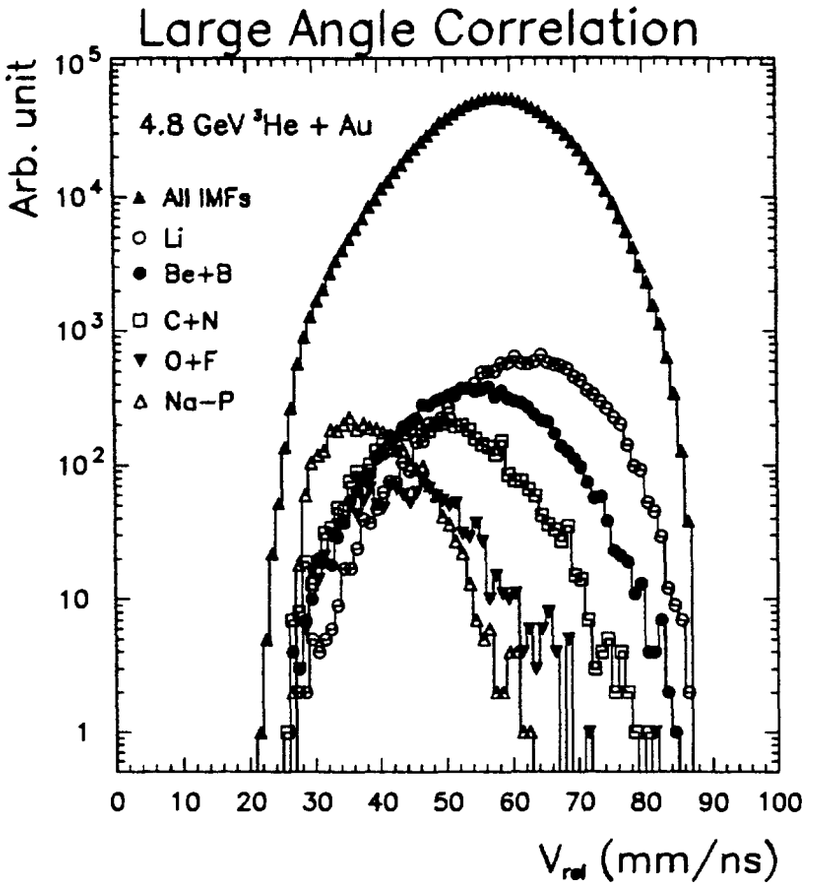

Figure 3: Relative velocity distribution for IMF pairs with $Z_1 = Z_2$. Data are for 4.8 GeV ^{3}He + ^{197}Au reaction. Upper curve is for all IMF pairs.

assumes time-dependent emission from an expanding source prior to breakup, whereas the latter describes a source undergoing simultaneous breakup. In order to emphasize the possible influence of time-dependent emission, the default conditions of both codes have been employed; i.e. K=144 MeV for EES and $\rho/\rho_o \sim 1/3$ and no prequilibrium emission for SMM. In order to account for the distribution of residue masses and excitation energies, identical INC results[4] for these systems were used as input to the EES and SMM calculations.

The INC/EES and INC/SMM calculations are compared with the data in Fig. 4. For the INC/EES model there is generally good agreement with the data, especially for the ^{197}Au target. In contrast, the slope of the INC/SMM model diverges well below the data for low-Z IMFs. The difference between the model predictions can be understood as follows. If the emission process is time-dependent, IMFs emitted early in the expansion phase will be more energetic due to the larger temperature, charge and density of the source, plus any expansion boost the fragment may receive. The results are consistant with a model in which light fragments are emitted early in the expansion stage. This "preequilibrium IMF" aspect of the disassembly mechanism is present in the EES model, but not in SMM. [While a prequilibrium option can be implemented in the SMM code of Ref. 13, it accounts only for LCPs and hence would not affect the present results.] For the heaviest fragments both models and the data are in general agreement, suggesting that the final breakup stage of the reaction can be satisfactorily described by both the SMM and EEs models.

4 The "Caloric Curve"

Recently, Pochodzalla *et al.*,[14] have reported evidence for the existence of a "caloric curve" in studies of peripheral ^{197}Au + ^{197}Au collisions at 600 MeV/A bombarding energy. These results trace the temperature, determined by the isotope-ratio technique,[15] as a function of the excitation energy per nucleon of the hot, fragmenting residues. A plateau is observed in this temperature/heat content diagram, suggestive of a phase transition from the nuclear liquid to a nucleon gas.

A similar curve[16] has been constructed for the 4.8 GeV ^{3}He + ^{197}Au system, using a ^{2}H/^{3}H and ^{3}He/^{4}He thermometer, where

$$T_{\mathrm{HHe}} = \frac{14.3\mathrm{MeV}}{[1.6\mathrm{R(H)/R(He)}]}. \qquad (3)$$

Here, R(H) = Y(^{2}H)/Y(^{3}H) and R(He) = Y(^{3}He)/Y(^{4}He). In this analysis, T is calculated for two cases: (1) only thermal H and He isotopes are accepted,

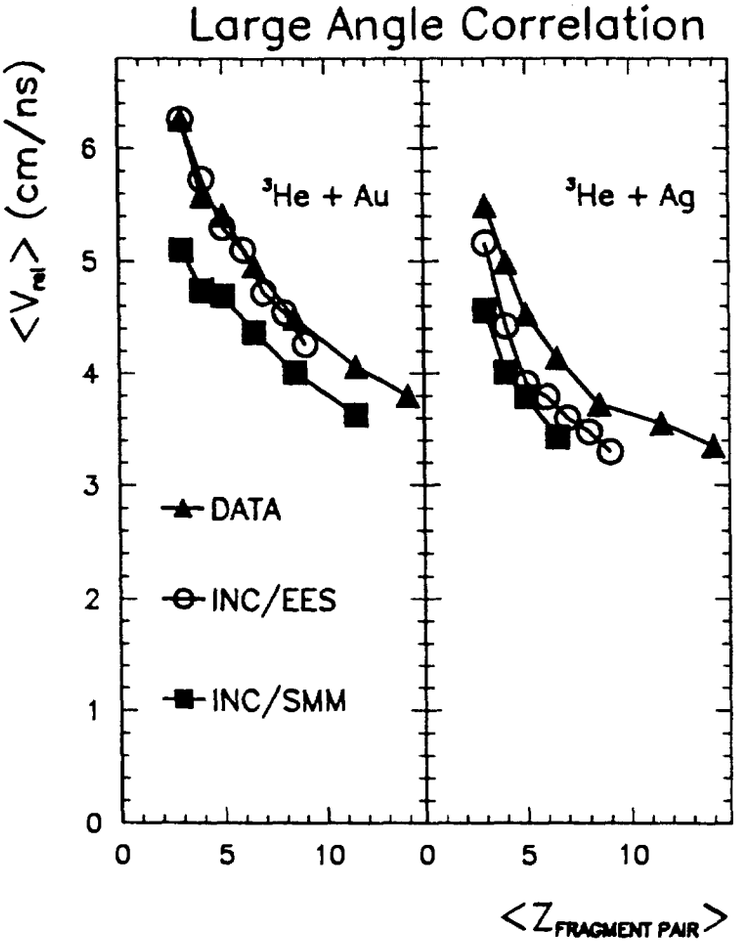

Figure 4: Average relative velocity for identical fragments as a function of fragment charge (triangle) for 4.8 GeV ^{nat}Ag (right) and ^{197}Au (left) targets. Open circles give predictions of the INC/EES calculation and squares show INC/SMM predictions.

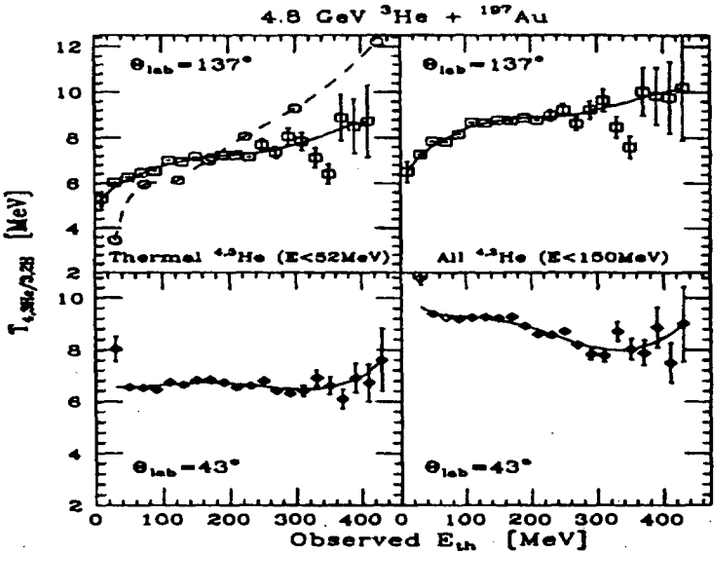

Figure 5: Temperatures determined from double isotope ratios of thermal ^{3}He/^{4}He and d/t plotted as a function of thermal energy. Left panel: temperatures determined using light-ion double-isotope ratios, T_{ratio}, when only the thermal helium isotopes energy range (38 to 52 MeV) is used in the ratios for the reaction of 4.8 GeV ^{3}He on gold. Right panel: T_{ratio} determined as in the left panel except including the energy range of helium isotopes from 38 to 140 MeV. Circles are slope temperatures at 137° for thermal ^{4}He.

and (2) the full H and He measured spectra are included; no corrections have been made for sequential decay.

In Fig. 5, the isotope-ratio temperature T_{HHe} for the 4.8 GeV ^{3}He + ^{197}Au reaction is plotted versus the measured thermal energy, which is proportional to the excitation energy of the system, as discussed above. For reference, an observed thermal energy of 500 MeV corresponds to a total excitation energy of $E^* \approx 1500$ MeV or $E^*/A_{residue} \approx 9$ MeV/nucleon.[2] Fig. 5 shows an approximate plateau in the behavior of T_{HHe} as a function of E_{th}. However, the results are sensitive to the acceptance region of the ejectile energy spectrum and the angle of observation. When the full experimental H and He isotope spectra are included in the analysis, the plateau occurs in the vicinity of $T \approx 8$ - 9 MeV. For thermal ejectiles only, the plateau is near $T \approx 6.5$ - 7 MeV. Corrections for sequential decay should decrease these values.[17]

The shape of the curve also depends on the angle of observation. At backward angles, T_{HHe} increases with E_{th}, consistent with expectations and

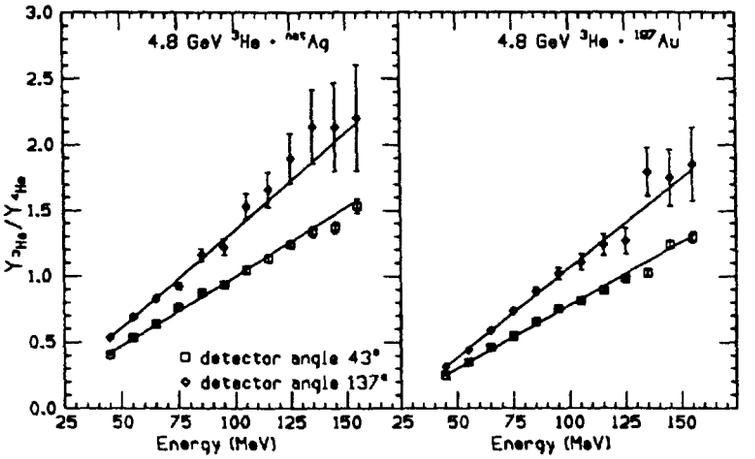

Figure 6: Plot of ^{3}He/^{4}He ratios as a function of particle kinetic energy at laboratory angles of 43° and 137°. The left panel is for the reaction of 4.8 GeV ^{3}He + ^{nat}Ag while the right panel is for the same projectile energy but using a ^{197}Au target. The solid lines are linear fits to the data.

the data of Ref. 14. However, at forward angles, the temperature actually increases at low E_{th} values. This behavior is best understood as due to the effects of nonequilibrium emission, which is most prominent at forward angles and for low E_{th} values (i.e. peripheral collisions). Studies at lower bombarding energies have shown that the ^{3}He/^{4}He ratio increases strongly with increasing ejectile kinetic energy.[18] This is illustrated for the 4.8 Gev + ^{197}Au data in Fig. 6, where the ^{3}He/^{4}He ratio is plotted as a function of fragment energy, showing increases of a factor of 4 - 6 over the measured energy range. These results emphasize the need to understand the emitting source fully in applying isotope ratio thermometer analyses of such data.

Also plotted in Fig. 5 are slope temperatures calculated from the spectra of ^{4}He observed at backward angles. At relatively low values of E_{th}, these track consistently with the data. A plateau is also observed, but over a narrower range of thermal energy before the temperature begins to increase strongly for the most violent collisions.

5 Summary

Studies of light-ion-induced multifragmentation have been performed on the 1.8 - 4.8 GeV ^{3}He + Ag, Au systems with the ISiS 4π detector array. The

data indicate a saturation in deposition energy near 4 GeV for the ^{3}He + Ag system and also illustrate the importance of nonequilibrium effects in evaluating the excitation energy of the source. Fragment-fragment correlations and relative velocity distriubutions suggest a scenario in which multifragmentation is a rapid, $\ll$ 100 fm/c, time-dependent phenomenon. Light fragments are preferentialy emitted as the residue expands and cools, followed by near-simultaneous breakup of the most highly excited residues. Examination of isotope-ratio temperatures (and spectral slope temperatures) as a function of thermal energy exhibit a plateau that is dependent on angle of observation and the fragment energy acceptance.

Acknowledgments

We acknowledge the contribution of W.A. Friedman, A. Botvina, H. Breuer, N.R. Yoder and J. Brzychczuk to various parts of this work. Primary funds for this research were provided by the US DOE; additional support was provided by the US NSF, NSERC (Canada) and CEA (France).

References

1. K. Kwiatkowski *et al.*, *Nucl. Instrum. Methods* **360**, 571 (1995).
2. K.B. Morley *et al.*, *Phys Lett. B* **355**, *52 (1995)*; *Phys. Rev. C*, in press.
3. K. Kwiatkowski *et al.*, *Phys. Rev. Lett.* **74**, 3756 (1995).
4. Y. Yariv and Z. Fraenkel, *Phys. Rev. C* **24**, 488 (1981).
5. P. Danielewicz, *Phys. Rev. C* **51**, 716 (1995).
6. W. Bauer *et al.*, *Phys. Rev. C* **34**, 2127 (1986).
7. G. Wang *et al.*, *Phys. Rev. C* **53**, 1811 (1996).
8. V. Barashenkov *et al.*, *Sov. J. Nucl. Phys.* **13**, 422 (1971); V. Toneev and K.K. Gudima, *Nucl. Phys.* **400**, 173c (1982).
9.
10. W.A. Friedman, *Phys. Rev. C* **42**, 667 (1990).
11. J.P. Bondorf *et al.*, *Nucl. Phys. A* **443**, 321 (1985).
12. D.H.E. Gross, *Rep. Prog. Phys.* **53**, 605 (1990).
13. V.E. Viola *et al.*, Proc. Winter Workshop on Nucl. Dynamics, Snowbird UT, Jan. 1996 (eds. W. Bauer and G. Westfall), to be published.
14. A. Botvina *et al.*, *Nucl. Phys. A* **507**, 649 (1990); *Phys. At. Nucl.* **57**, 628 (1994).
15. J. Pochodzalla *et al.*, *Phys. Rev. Lett.* **75**, 1040 (1995).

16. S. Albergo *et al.*, *Nuovo Cimento* **89A**, 1 (1985).
17. D.S. Bracken, Ph.D. Thesis, Indiana University (1996).
18. M.B. Tsang *et al.*, these proceedings.
19. W. Skulski *et al.*, *Phys. Rev. C* **40**, 1279 (1989).